The Effect of Water Vapor on Oxidation Performance of Alloys Used in Recuperators

Bruce A. Pint, Karren L. More and Peter F. Tortorelli
Oak Ridge National Laboratory
Metals and Ceramics Division
Oak Ridge, Tennessee 37831-6156
Phone: (865) 576-2897, E-mail: pintba@ornl.gov

ABSTRACT

The use of a recuperator to recover waste heat from the exhaust gases is one method for improving a microturbine's energy efficiency. This study looked at the effect of water vapor in the exhaust gas on the oxidation resistance of a current technology stainless steel and several high performance replacement alloys. Alloys of interest are high-Cr, Ni-base superalloys such as alloy 625 and aluminum-containing alloys such as Haynes alloy 214 and Plansee alloy PM2000, which is an oxide-dispersed FeCrAl. The latter two alloys form a protective external alumina scale which is more resistant to water vapor environments than chromia scales. Scanning and transmission electron microscopy characterization of the specimen surface oxides after laboratory exposures showed only minor effects of the addition of water vapor to the environment, which is consistent with the excellent corrosion resistance of these high performance alloys.

INTRODUCTION

One concern about small (25-200kW) gas turbine engines (microturbines) is their relatively low (<30%) efficiencies.[1] Higher efficiencies would be attractive from both economic and environmental standpoints. A common strategy to improve efficiency is to employ a recuperator to use exhaust heat to preheat the inlet air to the combustor.[2,3] A variety of designs are being employed but, in order to maximize heat-transfer, most include some type of thin-sheet, corrugated metal. Currently, many designs employ stainless steel foils[4] which limits the operating temperature of the recuperator to approximately 600-650°C (1100-1200°F) due to creep and corrosion limitations. The pressure and temperature differentials between the incoming compressed air and the exhaust gas result in a stress on the foil and significant foil deformation would limit the performance of the recuperator. Corrosion also can cause failure of the foil components by reducing the load bearing cross-section. Of particular concern for corrosion is the presence of water vapor in the exhaust gas (as a combustion product). Water vapor is known to accelerate the oxidation rate of chromia-forming stainless steels[5-10] which would normally be very corrosion resistant at similar temperatures in dry air.

To further improve efficiency, it is necessary to increase the turbine rotor inlet temperature and/or pressure ratios. It also would be desirable to increase the maximum operating temperature of the recuperator. However, new recuperator materials are required to achieve the required durability (i.e. performance life) if higher operating temperatures are needed. Various high temperature alloys[10] and ceramics[11] have been investigated for such applications.

This study continues previous work[10] where creep and corrosion testing was performed on foil material (≈75-125μm or 3-5mil thickness) to select alloys for higher temperature (750°-1000°C, 1400-1800°F) recuperator performance. The objective of this work is to characterize the oxidation products on each of the candidate alloys in order to study the role of water vapor in the exhaust gas on the oxidation performance. Hopefully this will lead to a better understanding of the role of water vapor and aid in the design and development of low-cost oxidation resistant alloys for this application.

EXPERIMENTAL PROCEDURE

Both Ni- and Fe-base alloys were considered for this work but only those materials which demonstrated sufficient creep strength were included. Four alloys were selected for microstructural characterization: two chromia-forming alloys: (1) type 321 stainless steel and (2) Inconel 625; and two alumina- forming alloys: (3) Haynes alloy 214 and (4) PM2000, an oxide dispersion strengthened (ODS) FeCrAl alloy. Nominal chemical compositions are provided in Table I. Alloy 321 provides a baseline for current stainless steel performance in recuperators.

Long-term oxidation testing was performed on foil specimens, typically 100μm (4 mil) thick.[10] However, in order to simplify specimen preparation for the transmission electron microscope (TEM), 1mm thick specimens were polished to a 0.3μm finish and oxidized for characterization.

Long-term oxidation testing on foils was performed in tube

Table I. Nominal compositions (wt%) of the various alloys.

	Fe	Ni	Cr	Al	Other
Type 321	bal.	11	17		0.3Ti
Alloy 625	4	bal.	21		9Mo, 4Nb
Haynes 214	3	bal.	16	4	0.1Zr, Y
Plansee PM2000	bal.		19	5	Ti, Y_2O_3

furnaces. For testing in air, the alumina furnace tubes were not sealed and the specimens were sometimes placed into annealed alumina crucibles with lids to collect any spalled oxide. For testing in air plus 10% (by volume) water vapor, the foil specimens were placed in annealed alumina racks to hold the specimens upright and allow the humid air to flow among the specimens. The ends of the alumina tube were sealed and the water vapor was controlled by a water injection system described elsewhere [8]. Specimens were approximately 2.5cm x 1.5cm and were tested with the as-rolled surface finish after ultrasonic cleaning in acetone and alcohol. Exposures were for 100h cycles at 700° and 800°C and specimens were weighed between cycles using a Mettler model AG245 balance.

For the 1mm thick specimens oxidized for shorter times for TEM analysis, exposures were conducted using a Cahn model 1000 microbalance to continuously monitor the mass change. Water vapor was added to this equipment by a similar gas system. For the alumina-forming alloys, exposures were made at higher temperatures (1000°-1100°C) to grow slightly thicker oxides. Scales formed on these alloys at lower temperatures were too thin to be characterized.

After exposure, specimens were characterized by scanning electron microscopy (SEM) in plan view and mounted in epoxy and polished metallographically in order to observe the oxide scale cross-section. For higher resolution work, TEM specimens were made using focused ion beam (FIB) thinning[12]. TEM characterization included microchemical analysis using energy dispersive x-ray (EDX) analysis on a scanning transmission electron microscope (STEM).

RESULTS

Long-Term Oxidation Exposures

To illustrate the relative oxidation behavior of the four alloys, some of the long-term exposure results are presented in Figure 1. The performance of type 321 stainless steel illustrates the concern about the effect of water vapor on the oxidation rate. In dry air at 800°C, Figure 1b, relatively low mass gains and little scale spallation were observed. With a nominal 17%Cr content (Table I), this alloy is expected to form a protective chromia scale at this and lower temperatures. Yet, in the presence of water vapor, this alloy exhibited significant mass gains at 700° and 800°C. The performance is summarized in Table II. The mass gain for type 321 alloy in water vapor was more than an order of magnitude higher than in air. The degree of attack meant that a large fraction of the foil was consumed in just 1000h.

In contrast, the alloy with a higher Cr content, alloy 625, or those which form alumina scales showed no strong adverse effect of adding water vapor to the test. At 700°C, very low mass gains were measured, Table II. At 800°C, alloy 625 showed no significant increase in mass gain with the addition of water vapor. A slightly higher mass gain was observed in dry air, but appeared to be anomalous.

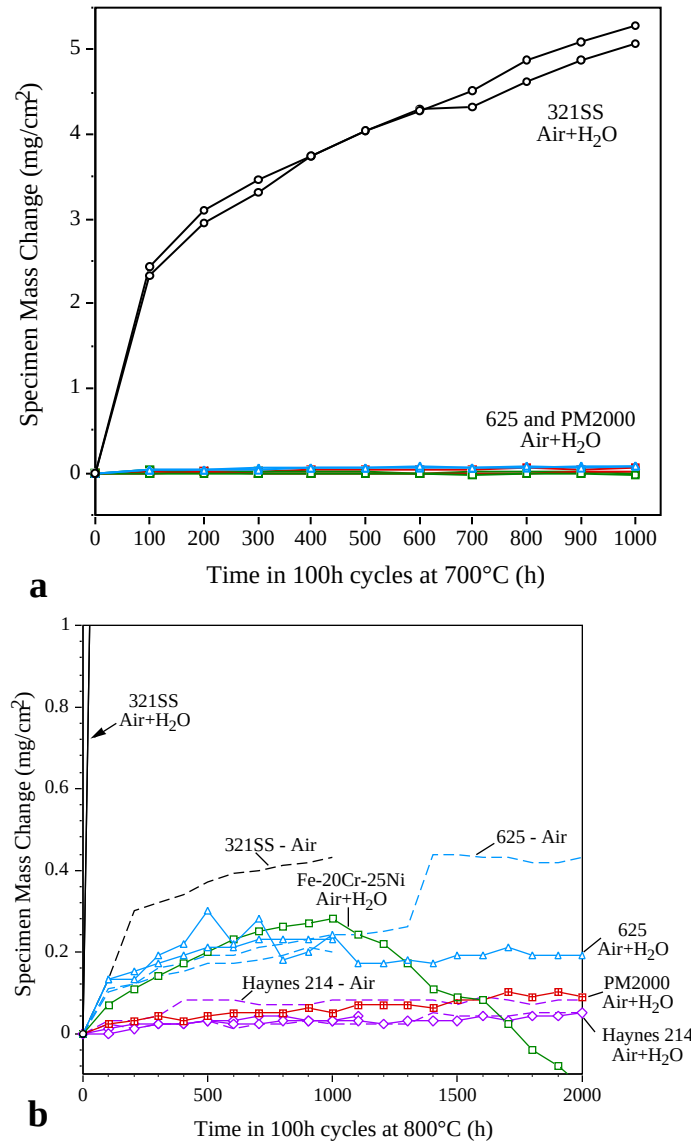

Figure 1. Oxidation data for 100-125μm (4-5mil) thick foils at (a) 700° in air with 10vol%H_2O and (b) 800°C with and without 10vol% H_2O. While Type 321 stainless steel was heavily attacked by the addition of water vapor, the other alloys were not as strongly corroded.

Table II. Specimen mass change of foil specimens after 10, 100h cycles at each condition.

Temperature	700°C	800°C	800°C
Water Vapor	10%	10%	0%
Type 321	5.18*	8.95*	0.43
Alloy 625	0.08*	0.24*	0.22*
Haynes 214	n.t.	0.03*	0.05*
Plansee PM2000	0.03	0.05	0.43

*average of two specimens exposed

At 800°C, even lower mass gains were measured for the alumina-forming alloys, Haynes 214 and PM2000. The growth rate of Al_2O_3 scales is significantly slower than Cr_2O_3 scales and alumina does not have a volatility problem like Cr_2O_3. These alloys performed well in humid air, with lower mass gains than those measured in dry air, Table II.

Scale Characterization on Type 321 Stainless Steel

Previous work has characterized the accelerated attack on a stainless steel with similar composition, type 347.[13] Nodules of iron oxides nucleated on the surface and grew with a duplex structure consisting of an outer iron oxide with an inner mixed Fe and Cr oxide. The nucleation increased with increasing water vapor content or temperature.[8] In order to study the role of water vapor on the oxidation behavior of type 321 stainless steel, conditions were selected prior to the onset of accelerated attack. Specimens were oxidized for only 100h at 700°C with and without 10vol.% H_2O to characterize changes in the oxide scale with the addition of water vapor.

In both cases, the scale in plan view appeared similar with numerous nodules on the scale surface and no indication of scale spallation or cracking, Figures 2a and 2b. The nodules may be slightly smaller and less dense in the presence of water vapor but it was a minor difference. After these relatively short exposures, the scale was extremely thin and difficult to analyze in cross-section, Figures 2c and 2d. It was not possible to examine the thin scale using EDXin the SEM. The scale appeared slightly thinner in water vapor but the cracking of the oxide makes the comparison difficult. The scale also was too thin for x-ray diffraction analysis. A previous study of Fe-13Cr oxidized at 700°C detected $(Fe,Cr)_3O_4$ but not Cr_2O_3.[14]

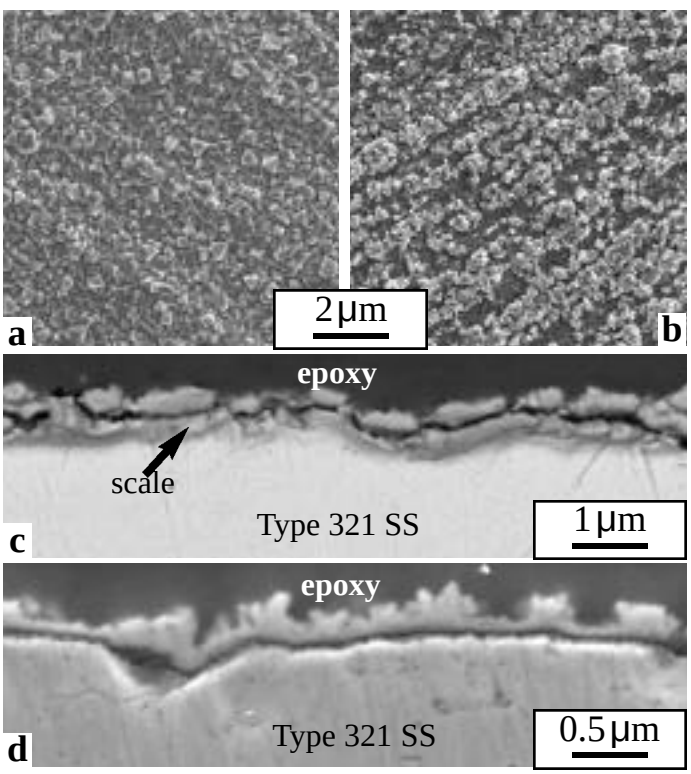

Figure 2. SEM plan view and cross-sectional images of the scale formed on type 321 stainless steel after 100h at 700°C in (a,c) air and (b,d) air plus 10% water vapor.

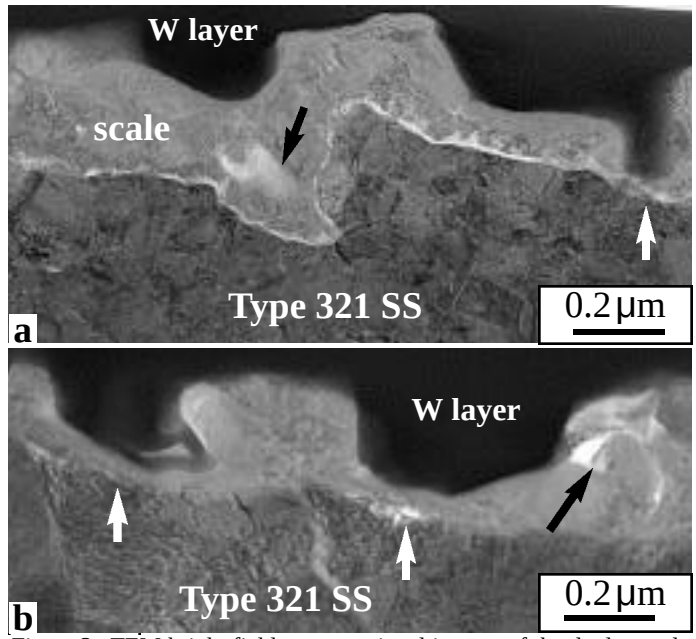

Figure 3. TEM bright field cross-sectional images of the duplex scale formed on type 321 stainless steel after 100h at 700°C in (a) air and (b) air plus 10%water vapor. During FIB specimen preparation, the outer surface is coated with a protective W layer.

Figure 3 shows TEM cross-sections of the scale formed on type 321 stainless steel. While it has been hypothesized that the addition of water vapor results in increased porosity or defects in the scale , there was little indication of such in these cross-sections. The primary difference appeared to be that the scale was thinner in regions between nodules when exposed to water vapor than in dry air., white arrows in Figure 3b. This difference may be due to CrO_3 or $CrO_2(OH)_2$ evaporation.[9] However, there were occasional thin areas for the scale grown in dry air, white arrow in Figure 3a. In these thin areas, the scale was rich in Cr. More Fe and Mn were observed in thicker areas and in the nodules. Relatively large Mn-rich oxides were observed in both scales, black arrows in Figure 3. Based on energy dispersive x-ray analysis, the Mn-rich particles had a Cr:Mn:Fe composition ratio of 4:2:1.

In order to better illustrate the microchemical analyses, high-resolution STEM x-ray maps were made in regions of both specimens. The box in Figure 4a shows the region analyzed from the scale formed in humid air. After these oxidation conditions, both Mn and Ti were observed in the oxide layer of both specimens. A large Mn-rich precipitate was observed as well as smaller Ti-rich oxide particles. An x-ray peak overlap occurs between Ti and W, thus a false Ti signal occurs in the W layer, which was deposited during specimen preparation. The thin section on the right side of the scale was rich in Cr. Based on these analyses, there is no clear difference in chemical composition between the two scales. The most significant difference with the addition of water vapor may be the scale thickness but due to the oxide nodules, this difference was difficult to quantify.

Scale Characterization on Alloy 625

Because of its superior performance, specimens of alloy 625 were oxidized with and without water vapor for 100h at 700° and 800°C.

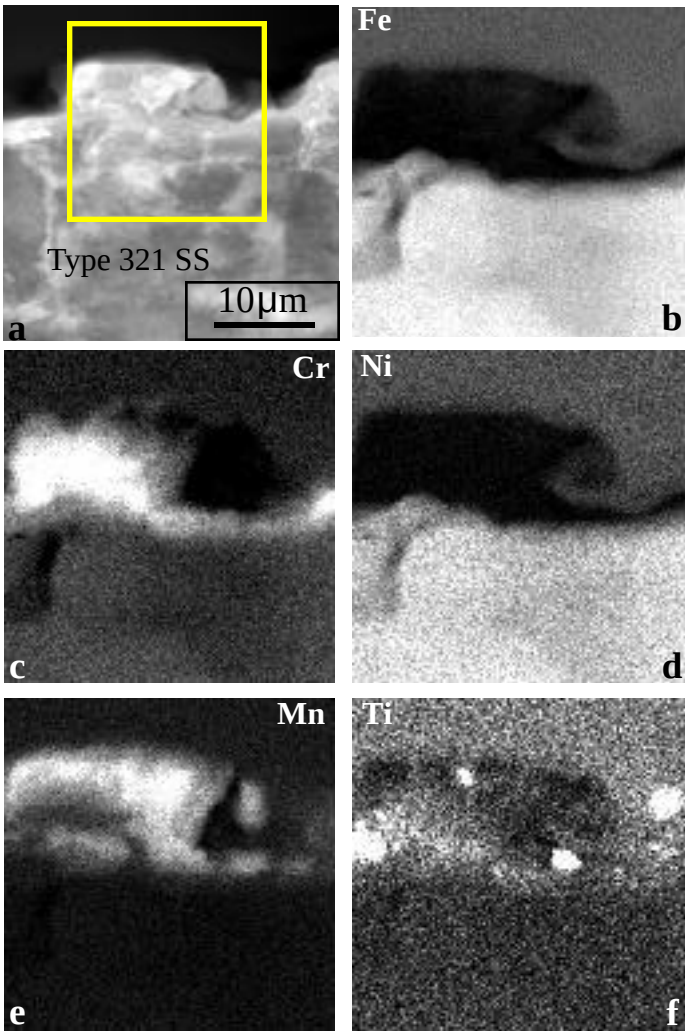

Figure 4. (a) STEM bright field cross-sectional image of the scale formed on type 321 stainless steel after 100h at 700°C in air plus 10% water vapor. X-ray maps for the box in (a): (b) Fe, (c) Cr, (d) Ni, (e) Mn and (f) Ti.

Water vapor did not appear to significantly affect the performance of this alloy at either temperature, perhaps due to the higher Cr content. As with type 321, the scale formed after 100h at 700°C was extremely thin, Figures 5a and 5b. Because of the Mo and Nb additions, this material has some distinctive features in the metal. Round precipitates rich in Mo and acicular particles rich in Nb formed in the metal near the scale interface during exposure. They appear lighter due to atomic number contrast in the SEM back-scattered electron image. Again because of cracking of the thin oxide, it was difficult to characterize the scale microstructure using SEM. As with type 321 stainless steel, the scale formed on alloy 625 appeared somewhat thinner when grown in humid air, possibly due to evaporation. With the addition of water vapor, there also appeared to be more precipitates in the metal.

At 800°C, the scale was somewhat thicker and better developed, Figures 5c and 5d. The particles in the metal were larger than those formed at 700°C. At this temperature, the scale formed on alloy 625 appeared thicker in humid air. This suggests that any loss in thickness due to evaporation was compensated by a faster scale growth rate.

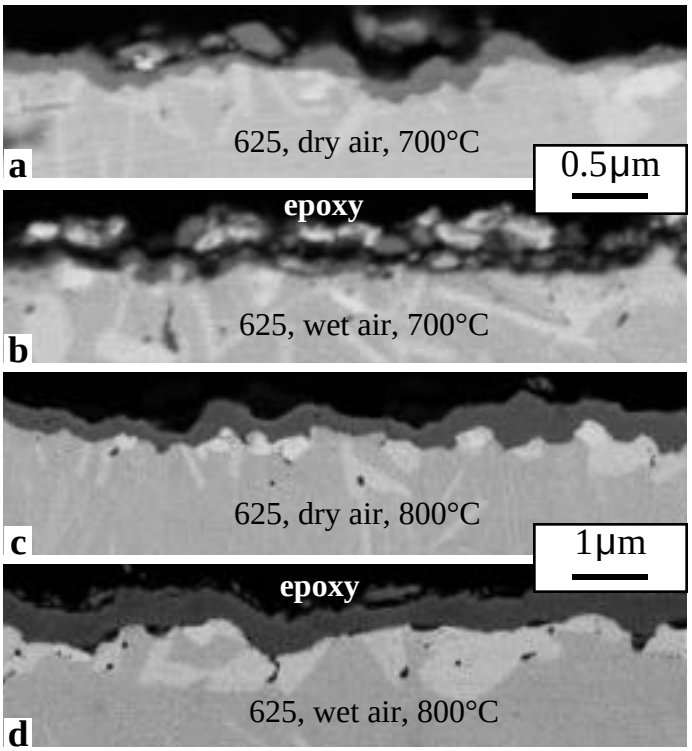

Figure 5. SEM back-scattered electron images of polished cross sections of the scale formed on alloy 625 after 100h at (a,b) 700°C and (c,d) 800°C in (a,c) air and (b,d) air plus 10%water vapor. The round precipitates in the metal are rich in Mo and the acicular precipitates are rich in Nb.

Similar to the observation at 700°C, there appear to be more particles in the metal for the specimen grown in water vapor. If the particles form due to selective oxidation of Cr, leaving Mo and Nb enriched in the metal, then the higher density of particles may suggest a faster Cr consumption rate in the presence of water vapor. The long-term oxidation behavior of alloy 625 showed a slight mass loss in air with water vapor compared to that in dry air. Because the scale was continually evaporating, a faster Cr consumption rate would be expected with water vapor. There also appears to more voids at the metal-scale interface and in the metal after exposure to water vapor. This suggests that possibly Mo was evaporating. However, exposure to water vapor did not lead to any increase in scale spallation.

Cross-sections for TEM analysis were prepared from the specimens shown in Figure 5. In Figures 6a and 6b, the scales formed at 700°C without and with water vapor are shown respectively. Assuming that these regions are representative of the two scales, the addition of water vapor resulted in a thinner scale. In this alloy, accelerated oxidation may have been avoided because of the higher Cr content or because the precipitates in the alloy provided interfaces for more rapid Cr diffusion. One interesting feature of the scale formed in water vapor was the presence of two large voids beneath the scale, Figure 6b. These voids appear too large to be accounted for by the loss of Cr into the scale. They do appear to be of similar size as the Mo-rich precipitates. They may have formed due to the evaporation of MoO_3 from beneath the oxide, possibly through a crack or other defect in the oxide. The voids also could be artifacts of specimen preparation but similar problems have not been observed for other cross-sectional

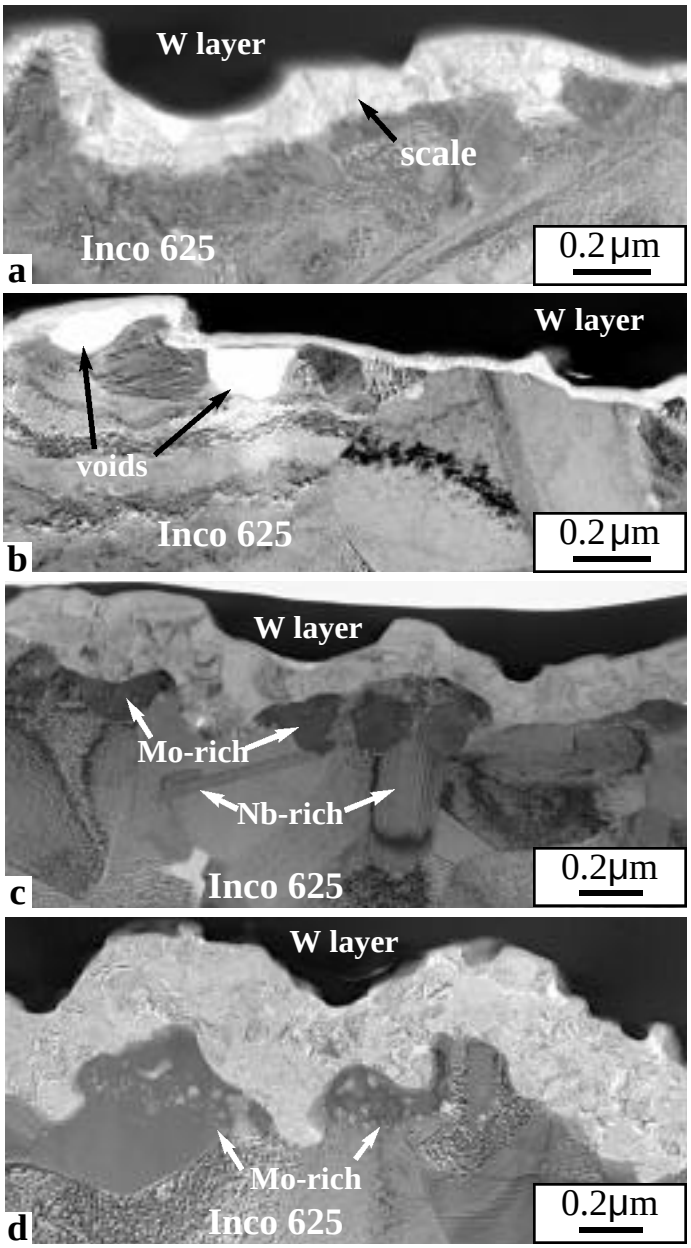

Figure 6. TEM bright field cross-sectional image s of the scale formed on alloy 625 after 100h at (a,b) 700°C and (c,d)800°C in (a,c) air and (b,d) air plus 10%water vapor. The round precipitates in the metal are rich in Mo and the acicular precipitates are rich in Nb.

scale specimens prepared by FIB milling. Another interesting feature in these cross-sections is the presence of very small voids in the Mo-rich particles. This is observed under all exposure conditions, but are easiest to see in Figure 6d.

The cross-sections of the scales formed after 100h at 800°C revealed many of the same features observed at 700°C but larger in size, Figures 6c and 6d. The major difference is that the scale was thicker when exposed to water vapor. It also appears that there is a higher density of voids in the Mo-rich phase after exposure to water vapor. Preliminary results indicate that the Mo-rich precipitates in the metal are predominantly Mo and Ni, but only limited chemical analysis of these specimens has been completed at this time. No information is available on the presence of a sub-layer silica scale[14] or which elements besides Cr are enriched in the oxide scale.

Scale Characterization on Haynes 214

A previous paper provided some characterization information on the scale formed on Haynes 214.[10] Because of the extremely thin alumina scales formed even at 900°C, the scale was characterized after 100h at 1100°C with and without 10%H_2O to examine the role of water vapor. Similar to the results at 800°C (Figure 1b and Table II), the addition of water vapor did not significantly change the mass gain at 1100°C, however, a slightly higher transient mass gain was noted. Metallographic cross-sections of the two specimens showed only a slightly rougher metal-scale interface with the addition of water vapor.

Figure 7 shows TEM images of the scales formed in dry and humid air. Both scales have an outer $Ni(Cr,Al)_2O_4$ layer with an inner α-Al_2O_3 layer. The Ni-rich layer forms initially but is eventually undercut by a continuous alumina layer. The outer layer has a relatively equiaxed grain structure while the inner layer has a columnar grain structure. The columnar grain structure is typically observed on alloys containing reactive elements,[15] in this case, Y and Zr. These elements were added to improve the alumina scale adhesion and reduce the scale growth rate. In both specimens, Y and Zr were found segregated to the Al_2O_3 grain boundaries, which also is typically observed.

At these oxidation conditions, the main effect of water vapor appeared to be a slightly greater total scale thickness, particularly in the transient Ni-rich oxide layer (white arrows in Figure 7). There also appeared to be more voids in the scale formed in water vapor, especially in the outer oxide and at the $Ni(Cr,Al)_2O_4$-Al_2O_3 interface (arrows in Figure 7b).

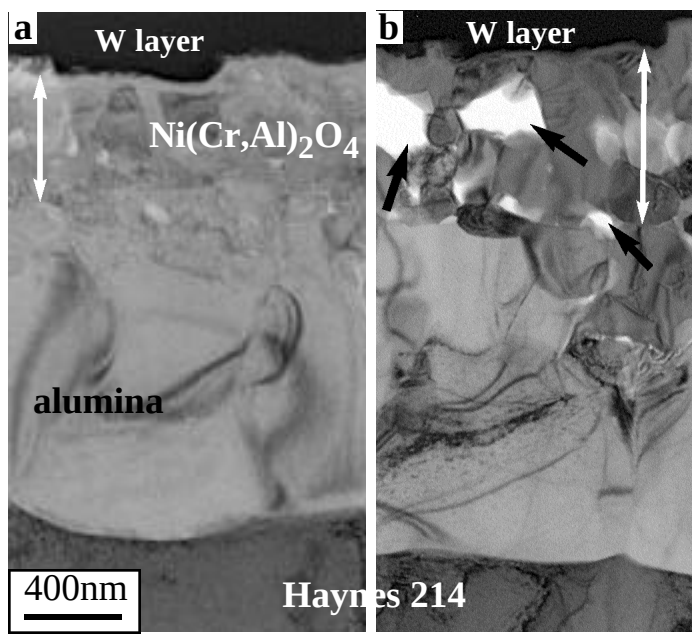

Figure 7. TEM bright field cross-sectional image of the duplex scale formed on Haynes 214 (NiCrAlFe+Y/Zr) after 100h at 1100°C in (a) air and (b) air +10%H_2O. Compared to the oxide formed in air, the oxide formed with water vapor was slightly thicker and contained more voids (arrows).

Scale Characterization on Plansee PM2000

Specimens of PM2000 were oxidized at 1000°C for 100h with and without water vapor. The addition of water vapor did not substantially change the total mass gain at this temperature and this was reflected in scales with similar thickness and grain structure, Figure 8. Similar to the scale formed on Haynes 214 at 1100°C, the alumina grain structure was mostly columnar with a few equiaxed grains near the gas interface. In the outer part of the scale, larger voids were observed in the scale formed in dry air with finer voids present in the scale grown in the presence of water vapor. In neither case were there significant voids observed in the inner portion of the scale.

Previous light microscopy did not reveal the formation of a transient oxide on this material after exposure to dry air.[10] However, SEM and TEM analysis (Figure 8a) showed a thin, continuous Fe- and Cr-rich layer about one grain thick. This transient oxide is similar to the Ni-rich oxide formed on Haynes 214. However, both analyses showed that the layer was not present when water vapor was added, Figure 8b. The difference is attributed to increased volatilization of CrO_3 or $CrO_2(OH)_2$ with the addition of water vapor. In both cases, a transient oxide would be expected to form but in one case the layer evaporates more quickly than in the other.

Unfortunately, neither of the TEM sections was near an oxide protrusion that was observed in the metallographic cross-sections.[10] Another difference between the two microstructures was finer grain diameters in the columnar scale formed in water vapor. This could be an important difference because a finer grain spacing results in a higher density of diffusion paths potentially resulting in a faster scale growth rate. However, it is possible that the grain size difference is only a localized occurrence.

In order to confirm the 100h observations, 500h oxidation experiments with and without water vapor also were performed at 1000°C. Again, the addition of water vapor did not appear to have a significant effect on the scale growth rate. TEM cross-sections of the two specimens are shown in Figure 9. The cross-section in Figure 9b happened to be in a region where the scale was convoluted and did not reflect an overall rougher oxide formed in water vapor. As was observed after 100h, the scale grown in dry air for 500h had an outer Fe- and Cr-rich layer while the scale grown in humid air did not. Unlike after 100h, the alumina columnar grain structure was very similar on both specimens. This is consistent with the similar growth rate observed in these two environments. In general, the addition of water vapor did not have a major effect on the scale microstructure formed on PM2000 at this temperature.

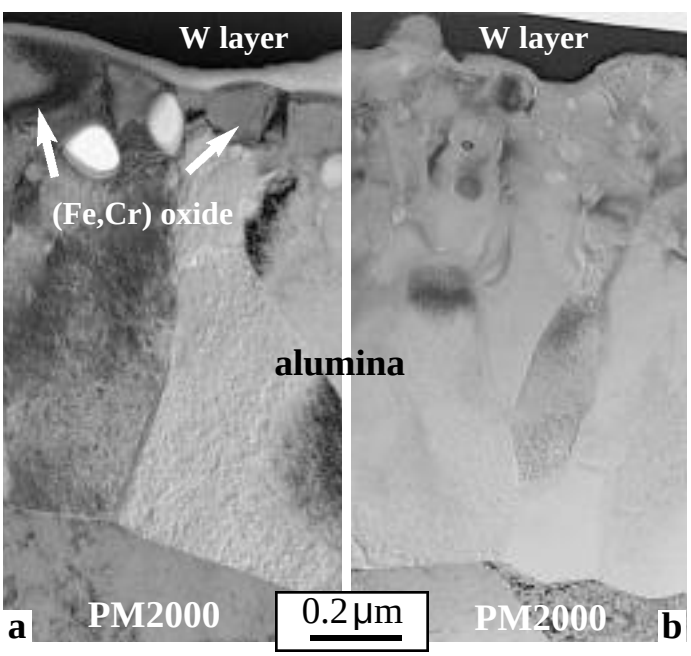

Figure 8. TEM bright field cross-sectional image of the duplex scale formed on PM2000 after 100h at 1000°C in (a) air and (b) air plus 10% water vapor. A Fe- and Cr-rich oxide was only detected for the scale formed in air.

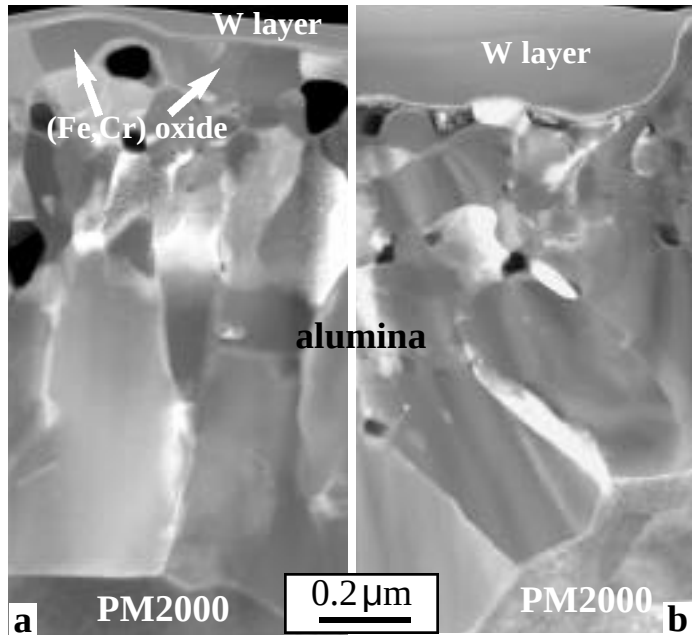

Figure 9. STEMannular dark field cross-sectional images of the duplex scale formed on PM2000 after 500h at 1000°C in (a) air and (b) air plus 10%water vapor. A Fe- and Cr-rich oxide was only detected for the scale formed in air.

DISCUSSION

One of the goals of the characterization work was to obtain a better understanding of the water vapor effect on protective oxide formation. The importance of water vapor in the environment has been known for more than 40 years but until recently, the problem had been largely ignored. It is now of significant importance as materials are needed which are oxidation resistant in water-laden environments. Unfortunately, there are no well-accepted mechanistic models to explain this effect. Therefore, it is not known when an effect of water vapor may appear. While this paper presents no significant new discovery regarding the effect of water vapor, it does provide some important baseline information from which to build a better understanding of the effect of water vapor.

In general, the addition of water vapor appeared to have only minor effects on chromia and alumina scale microstructures. For chromia-formers, a somewhat thinner scale was observed with the addition of water vapor after 100h at 700°C on type 321 stainless steel and alloy 625. At 800°C, on alloy 625, the scale was thicker with the addition of water vapor. The higher scale growth rate combined with

the volatilization of CrO_3 or $CrO_2(OH)_2$ suggests a higher Cr consumption rate in the presence of water vapor. A higher Cr consumption rate with a lower Cr content, like that found in type 321 stainless steel, may lead to accelerated attack. It also may represent a long-term problem for higher Cr content alloys as they become depleted in Cr during long-term exposures. Alloy 625 foil (100μm thick) showed low mass losses for 6,000 h at 800°C in air plus 10% H_2O. However, modeling longer oxidation times or predicting the oxidation-limited lifetime requires numerous assumptions about the failure criteria that are not well understood. A better understanding of the performance limitations of alloy 625 may assist in the design of lower cost alloys.

For alumina-formers, only minor changes were observed with the addition of water vapor, mostly associated with transient oxidation. The characterization results presented in this study are for higher temperatures than would be used in thin-walled recuperators but mass change results for 700°-900°C did not find any effect of water vapor on oxidation behavior out to 6000h. There is still some uncertainty associated with longer-term effects of exposure to exhaust gases but, without the evaporation problem associated with chromia scales, catastrophic problems appear less likely for these materials. Most likely, thin walled components could operate for extended periods at 900°C.

A final point that has not yet been considered is the combined effect of oxidation and stress. An applied tensile stress may cause periodic cracking of the scale leading to localized accelerated attack and loss of cross-section that may lead to early creep failure. Current creep testing is being conducted in air but future testing may be performed in a water vapor environment in order to examine this effect. Examining the scale after exposure to both stress and water vapor would give the best indication of any potential problems.

SUMMARY

The scale microstructures of four alloys was examined after oxidation with and without water vapor in the environment. In general, characterization of the corrosion products did not reveal any significant changes in the oxide scale microstructure due to the addition of water vapor. Minor changes in thickness were observed for chromia-forming scales with thinner scales forming in the presence of water vapor at 700°C (likely due to $CrO_2(OH)_2$ volatilization) and thicker scales at 800°C. Thinner chromia scales on stainless steel may be less protective leading to accelerated attack.

For alumina scales, only minor effects associated with transient oxides were observed. Alumina scales appear to be less susceptible to water vapor effects and are less likely to suffer accelerated attack due to its presence. If higher operating temperatures are required from recuperators to improve the efficiency of microturbines, it is likely that alloys with higher Cr contents or the ability to form an alumina scale will be required.

ACKNOWLEDGMENTS

The authors would like to thank M. Howell, G. Garner, K. S. Trent and D. Coffey at ORNL for assistance with the experimental work. This research was sponsored by the U.S. Department of Energy, Office of Power Generation Technology, Distributed Energy Research program under contract DE-AC05-00OR22725 with UT-Battelle, LLC.

REFERENCES

1. Energetics, Inc., 1999, “Summary of the Microturbine Technology Summit,” Report No. DOE/ORO 2081, Oak Ridge, TN.
2. Watts, J. H., 1999, “Microturbines: A New Class of Gas Turbine Engine,” Global Gas Turbine News, **39**(1), pp.4-8.
3. Hamilton, S. L., 1999, “Microturbines Poised to Go Commercial,” Modern Power Systems, **19**(9), pp.21-22.
4. Ward, M. E., 1995, “Primary Surface Recuperator Durability and Applications,” Report No.TTS006/395, Solar Turbines, Inc., San Diego, CA.
5. Caplan, D. and Cohen, M., 1959, "High Temperature Oxidation of Chromium-Nickel Steels," Corrosion, **15**, pp.57-62.
6. Quadakkers, W. J. and Ennis, P. J., 1998, "The Oxidation Behavior of Ferritic and Austenitic Steels in Simulated Power Plant Service Environments," Materials for Advanced Power Engineering 1998, J. Leconte-Beckers, F. Schubert and P. J. Ennis Eds, Forschungszentrum, Jülich Germany, pp.123-38.
7. Nickel, H., Wouters, Y., Thiele, M. and Quadakkers, W. J., 1998, "The Effect of Water Vapor on the Oxidation Behavior of 9%Cr Steels in Simulated Combustion Gases,” Fresenius Journal of Analytical Chemistry, **361**, pp.540-4.
8. Pint, B. A. and Rakowski, J. M., 2000, “Effect of Water Vapor on the Oxidation Resistance of Stainless Steels,” NACE Paper 00-259, Houston, TX, presented at NACE Corrosion 2000, Orlando, FL, March 2000.
9. Asteman, H., Svensson, J.-E., Norell, M. and Johansson, L.-G., 2000, “Influence of Water Vapor and Flow Rate on the High-Temperature Oxidation of 304L; Effect of Chromium Oxide Hydroxide Evaporation,” Oxidation of Metals, **54**, pp.11-26.
10. Pint, B. A., Swindeman, R. W., More, K. L. and Tortorelli, P. F., 2001 "Materials Selection for High Temperature (750°-1000°C) Metallic Recuperators for Improved Efficiency Microturbines," ASME Paper #2001-GT-445, presented at the International Gas Turbine & Aeroengine Congress & Exhibition, New Orleans, LA, June 4-7, 2001.
11. Omatete, O., Maziasz, P. J., Pint, B. A. and Stinton, D. P., 2000, “Recuperators for Advanced Microturbines,” Report No.ORNL/TM-2000/304, Oak Ridge National Laboratory, Oak Ridge, TN.
12. More, K. L., Coffey, D. W., Pint, B. A., Trent, K. S. and Tortorelli, P. F., “TEM Specimen Preparation of Oxidized Ni-Based Alloys Using the Focused Ion Beam (FIB) Technique,” (Presented at Microscopy & Microanalysis 2000, Philadelphia, PA, Aug. 2000).
13. Rakowski, J. M. and Pint, B. A., 2000, “Observations on the Effect of Water Vapor on the Elevated Temperature Oxidation of Austenitic Stainless Steel Foil,” NACE Paper 00-517, Houston, TX, presented at NACE Corrosion 2000, Orlando, FL, March 2000.
14. Hoelzer, D. T., Pint, B. A., Wright, I. G., 2000, "AMicrostructural Study of the Oxide Scale Formation on an ODS Fe-13Cr Alloy," Journal of Nuclear Materials, **283-287**, pp.1306-10.
15. Pint, B. A., 1996, ‘“Experimental Observations in Support of the Dynamic Segregation Theory to Explain the Reactive Element Effect,” Oxidation of Metals, **45**, pp.1-37.
16. Quadakkers, W. J., Elschner, A., Speier, W. and Nickel, H., 1991, “Composition and Growth Mechanisms of Alumina Scales on FeCrAl-based Alloys Determined by SNMS,”Applied Surface Science, **52**, pp.271-87.